Wear 303 (2013) 334–342

Contents lists available at SciVerse ScienceDirect

Wear

journal homepage: www.elsevier.com/locate/wear

Investigation on the fretting fatigue behaviors of steel wires under different strain ratios

De-kun Zhang [a,*], Hao Geng [a], Ze-feng Zhang [a], Da-gang Wang [b], Song-quan Wang [b], Shi-rong Ge [b]

[a] School of Materials Science and Engineering, China University of Mining and Technology, Xuzhou 221116, China
[b] School of Mechanical and Electrical Engineering, China University of Mining and Technology, Xuzhou 221116, China

ARTICLE INFO

Article history:
Received 30 December 2012
Received in revised form
24 March 2013
Accepted 25 March 2013
Available online 6 April 2013

Keywords:
Steel wire
Fretting fatigue
Fatigue life
Strain ratio
F_t–D–N curve

ABSTRACT

The fretting fatigue tests of steel wires were performed on the self-made fretting fatigue test equipment under different strain ratios ranging from 0.90 to 0.70 with contact loads of 50 N and 70 N. Curves of F_t–D–N were drawn, and the dissipated energy was calculated through the curves of F_t–D. Morphological features of fretting scar and fracture surface were observed by scanning electron microscopy (SEM). The results reveal that as the strain ratio decreased, the fretting regime changed from partial slip regime to mixed regime and slip regime. Shorter fretting fatigue life, higher wear coefficient were induced by a lower strain ratio. The curves of dissipated energy corresponding to three kinds of fretting regimes were different from each other. Morphologies of adhesive wear, abrasive wear and fatigue wear as well as accumulation of plastic deformation and micro-cracks were observed in fretting scars. All fatigue fractures in different fretting regimes could be divided into three regions.

1. Introduction

Fretting is a very small amplitude movement in the vibration environment that occurs between two approximately tight contact surfaces; at the same time, fatigue crack originated from the fretting area under alternating load will result in components that appear in the fretting fatigue phenomenon when the alternating stress is lower than the material fatigue limit [1,2]. During the usage process, the steel wire rope is affected by the axial stress and bending stress, which will cause fretting wear [3,4] to occur between wire and wire, strand and strand. Eventually the steel wire rope will be a failure attributing to fretting fatigue, which affects the normal operation of the equipments and mining safety production [5]. Fretting fatigue may accelerate the occurrence of crack initiation and propagation on the surface of the fretting component, and significantly reduce the fatigue life, which can cause disastrous consequences. Therefore, research on fretting fatigue problem has a great significance to improve the life and reliability of the steel wire rope.

Many researchers [6–12] carried out a great deal of researches on fretting fatigue behaviors of Ti–6Al–4V material. Zhou et al. [13,14] examined fretting wear behaviors of cables and fretting fatigue behaviors of a single aluminum wire, and thought that material plastic deformation, wear and fatigue crack initiation caused by fretting were the main reason of cable fatigue failure, and elaborated on four fretting maps about fretting fatigue and wear [15]. Ding et al. [16] proposed two impact parameters, the fretting condition and surface damage after fretting, respectively, to predict fretting fatigue behaviors. Neslen et al. [17] evaluated the fretting damage degree through the analysis of fretting surface topography, and found that when adhesion and slip coexist, fretting fatigue damage parameters presented a growth trend as the fretting cycles increased, and thermal imaging technology could effectively monitor cracks above 200 μm formed by fretting. Wang et al. [18] examined steel wire fretting fatigue behaviors under low cycles and different strains, and found that as the strain increased, the tangential force increased and the corresponding fretting fatigue life reduced. Steel wire fretting fatigue behaviors are influenced by many factors. However, reports on steel wire fretting fatigue behaviors are few. This study will mainly carry out wire fretting fatigue experiments and explore the effects of the strain ratio on steel wire fretting wear and fatigue behaviors. Moreover, such a study will provide useful information about the reliability of wire ropes in coal mines.

2. Experimental method

The cold drawing high quality carbon structure steel wires were chosen as the specimens in this research. The chemical

* Corresponding author. Tel.: +86 51683591918; fax: +86 51683591916.
E-mail addresses: dkzhang@cumt.edu.cn, dkzhang98@163.com (D.-k. Zhang).

0043-1648/$ - see front matter © 2013 Elsevier B.V. All rights reserved.
http://dx.doi.org/10.1016/j.wear.2013.03.020

Table 1
Chemical composition of wire specimens (wt%).

Composition	Fe	Mn	Si	Ni	C	S	P
Percentage (%)	94.62	4.53	0.02	0.01	0.84	0.001	< 0.001

Table 2
Mechanical properties of the wire specimens.

Material	Tensile strength (MPa)	Yield strength (MPa)	Modulus of elasticity (MPa)	Percentage of elongation (%)
Steel wire in hoisting rope	1600	640	2.03 × 105	1.9

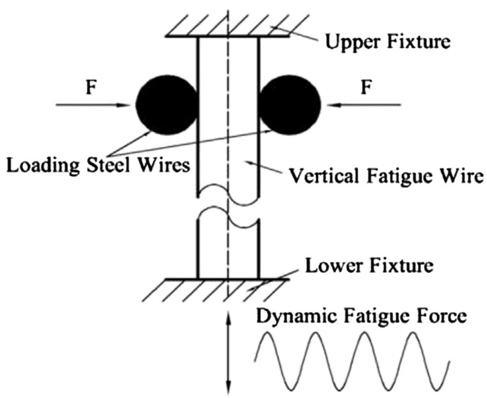

Fig. 1. Schematic diagram of the fretting fatigue principle.

Table 3
Fretting fatigue parameters of tensile steel wires.

Fatigue parameters		Fretting parameters	
Maximum fatigue strain, ε_{max}(%)	Cyclic frequency, f (Hz)	Strain ratio (r)	Contact load, F_n (N)
1.4	5	0.90, 0.85, 0.80, 0.75, 0.70	50, 70

composition and mechanical properties are listed in Tables 1 and 2, respectively. Tension–tension fretting fatigue tests were carried out on a self-made fretting fatigue experiment device mounted on a 20 kN computer controlled electro-hydraulic servo fatigue testing machine. Fig. 1 shows the schematic diagram of steel wire fretting fatigue, and the diameter of wire tension specimen is 1 mm with the length of 386 mm. The vertical tensile wire was fixed in the fatigue testing machine, and a certain value of strain was set. Each wire which provided contact loads was installed on fretting blocks which were on both sides of the vertical tensile wire with 90° contact angle. During the test, the reciprocating movement of fatigue testing machine piston makes the vertical tensile steel wire produce alternating strain, and thus fretting occurs in the contact area between loading wires and the vertical tensile wire, until the vertical tensile steel wire breaks down. When the position of the loading wire is fixed, through the regulation of fretting block, i.e. the height of fretting zone, the fretting amplitude of wires is regulated as the vertical tensile wire maximum strain and strain ratio are changed. Fretting fatigue parameters are shown in Table 3. The strain ratio is expressed as the following equation:

$$r = \sigma_{min}/\sigma_{max} \quad (1)$$

where r is the strain ratio, σ_{min} is the minimum fatigue stress of wire specimen, and σ_{max} is the maximum fatigue stress of wire specimen. It can be seen that as the strain ratio decreases, fretting amplitude between the steel wires increases. The friction force signal of tensile-compression force sensor recorded by dynamic signal analyzer and the displacement signal of the eddy current sensor were used for plotting fretting running characteristic curves, namely friction force the (F_t)–displacement–(D)-cycle(N) curves which helped identify the fretting regional characteristics and calculate the dissipation energy. The length and the width of wire wear scar were measured by the optical microscope with universal video imaging device; meanwhile, the maximum wear depth [19], wear volume and wear coefficient during the fretting fatigue process were also calculated. Using S-3000 scanning electron microscope (SEM) to observe morphologies of steel wire fretting fatigue and wear, the wear mechanism and its influence on fatigue life were explained.

3. Results and discussion

3.1. Fretting running characteristics

Fig. 2 shows the F_t–D–N 3D curves of steel wire under different strain ratios with the contact load of 50 N. The curves showed that different changing characteristics can be divided into three fretting running regions, i.e., partial slip regime, mixed slip regime and slip regime. When the ratio was 0.90 and fretting amplitude D of 66 μm, in addition to the early cycles, F_t–D curves always closed as linear, which meant the fretting ran in the partial slip regime (Fig. 2a), and it illustrated that the relative movement between contact surfaces mainly relied on elastic deformation of steel wire surface. When the ratios were 0.85 and 0.80 and fretting amplitudes D were about 0.95 μm and 125 μm respectively, the variation laws of F_t–D curves were the same, i.e., parallelogram in hundreds of cycles during initial fretting gradually closed into the elliptic form of the stable stage, which explained that fretting ran in mixed slip regime (Fig. 2b, c). Under the condition of ratios of 0.75 and 0.70, and the fretting amplitudes were 156 μm and 186 μm, respectively, F_t–D curves displayed parallelogram, explaining that fretting ran in slip regime (Fig. 2d, e), and completely relative slip happened between the steel wire contact surfaces.

Table 4 gives the fretting regime distributions of steel wires under contact loads of 50 N and 70 N and strain ratios of 0.90–0.70. It could be seen that as strain ratio decreased and fretting amplitude increased, fretting running regime changes from partial slip regime to mixed slip regime and slip regime, and relative slip between steel wire contact surfaces became easier. Larger contact load made relative slip between the contact surfaces more difficult; partial slip regime extended along the direction of larger fretting amplitude, and thus the slip regime was somewhat narrowed. The strain ratio and fretting amplitude appeared to be pushed back in mixed slip regime and slip regime. Under the condition of smaller amplitudes and larger contact load, fretting ran in the partial slip regime. However, when in larger amplitudes, relative slip between contact surfaces occurred easily and fretting was in the gross slip regime.

3.2. Friction coefficient and dissipation energy analysis

Fig. 3 shows the variation curves of friction coefficient under different strain ratios. At strain ratios of 0.80, 0.75 and 0.70, the friction coefficient curves can be divided into 4 stages: the